

# A comparison of frequentist and Bayesian inference: Searching for low-frequency p modes and g modes in Sun-as-a-star data

A.-M. Broomhall<sup>1\*</sup>, W. J. Chaplin<sup>1</sup>, Y. Elsworth<sup>1</sup>, T. Appourchaux<sup>2</sup>, R. New<sup>3</sup>

<sup>1</sup>*School of Physics and Astronomy, University of Birmingham, Edgbaston, Birmingham B15 2TT*

<sup>2</sup>*Institut d'Astrophysique Spatiale, CNRS-Université Paris XI UMR 8617, 91405 Orsay Cedex, France*

<sup>3</sup>*Faculty of Arts, Computing, Engineering and Sciences, Sheffield Hallam University, Sheffield S1 1WB*

4 February 2022

## ABSTRACT

We describe and use two different statistical approaches to try and detect low-frequency solar oscillations in Sun-as-a-star data: a frequentist approach and a Bayesian approach. We have used frequentist statistics to search contemporaneous Sun-as-a-star data for coincident, statistically-prominent features. However, we find that this approach leads to numerous false detections. We have also used Bayesian statistics to search for evidence of low-frequency p modes and g modes in Sun-as-a-star data. We describe how Bayesian statistics can be used to search near-contemporaneous data for coincident prominent features. Near-contemporaneous data were used to circumvent the difficulties in deriving probabilities that occur when common noise is present in the data. We find that the Bayesian approach, which is reliant on the assumptions made when determining the posterior probability, leads to significantly fewer false detections and those that are observed can be discredited using a priori knowledge. Therefore, we have more confidence in the mode candidates found with Bayesian statistics.

**Key words:** methods: data analysis, methods: statistical, Sun: helioseismology, Sun: oscillations

## 1 INTRODUCTION

Low-frequency p modes are expected to have very long lifetimes and so, if detected, their frequencies can be determined both accurately and precisely. This, in turn, makes low-frequency p modes important for constraining models of the structure of the solar interior. Only p modes with low degrees (low  $l$ ) travel through regions close to the solar centre and so observations of low- $l$  p modes are important for inferring the structure of the solar core. Mode amplitudes decrease with frequency and this, coupled with the increasing level of noise at lower frequencies, means that below  $1500\ \mu\text{Hz}$  oscillation signatures are difficult to detect. No independently confirmed detections of the core-penetrating, low- $l$  p modes have been made below  $\sim 970\ \mu\text{Hz}$  (e.g. García et al. 2001; Chaplin et al. 2002; Broomhall et al. 2007).

The large sound speed in the solar core means that the effect of core conditions on low-degree p modes is relatively small. On the other hand, solar gravity (g) modes, which have frequencies below  $450\ \mu\text{Hz}$ , are confined to the radiative interior and core, making them an extremely sensitive probe of the deep solar interior (see e.g. García et al. 2008; Mathur et al. 2008). Since g modes are evanescent outside the radiative interior their signatures are significantly attenuated by the time they reach the photosphere, where helioseis-

mic observations are made. It is, therefore, a major observational challenge to observe these modes. Appourchaux et al. (2010) is an up-to-date review of the current status of the search for g modes. García et al. (2007) claim to have found evidence of the signatures of g modes in data observed by the Global Oscillations at Low Frequencies (GOLF) instrument, onboard *Solar and Heliospheric Observatory (SOHO)*. García et al. (2008) found similar results when they examined 20 per cent more GOLF data than used by García et al. (2007). However, these results await independent confirmation and, to date, there have been no detections of individual g modes.

Some solar oscillations are thought to show a mixed character (e.g. Provost, Berthomieu & Morel 2000). They have a sensitivity to the Sun's internal structure that looks like a g mode, and so have excellent diagnostic potential, but they respond to surface conditions in a manner that is similar to p modes. Therefore, theoretically, mixed modes should be easier to detect than g modes, however, no mixed modes have yet been definitively identified. García et al. (2001) and Gabriel et al. (2002) tentatively identify one member of the  $n = 1, l = 1$  p mode, which is thought to be mixed. However, they are unable to determine which azimuthal component is detected.

Any signal from a low-frequency p mode (below  $1500\ \mu\text{Hz}$ ) or g mode is expected to be small compared to the surrounding background noise and so the following question arises: How does an observer decide whether a detection is real or not? This is

\* amb@bison.ph.bham.ac.uk

where statistical testing becomes important as it allows an observer to quantify the significance of any potential detection. To date the majority of statistical-based searches for low-degree p modes and g modes have taken a frequentist approach, i.e. it is common to determine the probability of observing a certain feature in a frequency-power spectrum based on the hypothesis that the spectrum contains pure noise. This is the H0 hypothesis. However, recent work by Appourchaux (2008) implies that the ‘*P* values’, which are quoted to assess the significance of a detection in a frequentist approach, may be too optimistic. It is, therefore, useful to also determine the probability of observing a feature in a frequency-power spectrum based on the alternative H1 hypothesis. The H1 hypothesis assumes that there is a signal in the data. However, to calculate this probability it is necessary to make certain *a priori* assumptions about the signal and so a Bayesian approach is appropriate. Appourchaux proposes that Bayesian statistics provides a more rigorous method of assessing the significance of any mode candidates than a frequentist approach. When using Bayesian statistics it is possible to use our knowledge of the structure of the Sun to put more constraints on the search for solar oscillations than when using a frequentist approach. In this paper we use both frequentist and Bayesian statistics to search for low-frequency p modes, g modes and mixed modes.

We have taken care to minimize the number of false detections. There are two ways in which false detections can be made. A type I error occurs when the null hypothesis is wrongly rejected. Here, that would mean wrongly rejecting the hypothesis that a prominent structure is due to noise. In other words a type I error would occur if we flagged a structure as a mode candidate when it is noise. A type II error occurs when the null hypothesis is not rejected when, in fact, it is false. In this paper that would mean accepting the hypothesis that a feature is due to noise when it is not. We regard type I errors as more serious than type II errors. Therefore we have decided to err on the side of caution and set very stringent requirements that need to be passed before a structure is considered as a mode candidate. For example, we require that any mode candidates be close to the mode frequencies predicted by solar models. While this restriction may increase the number of type II errors it is also likely to restrict the number of type I errors, which we consider to be more important.

The structure of this paper is as follows: we begin, in Section 2, with a comparison of the frequentist and Bayesian approaches. We then give a more detailed description of how frequentist statistics were used to search various data sets (Section 3). We have compared contemporaneous data for coincident features that are prominent when compared to the background noise. When determining the probability of observing such features in contemporaneous data, it is necessary to take account of any common noise that is present in the data due to, for example, the solar granulation. In order to do this Broomhall et al. (2007) derived a joint probability based on the assumption that the background noise has a Gaussian distribution, which is true in frequency-amplitude spectra. Therefore, when using the frequentist approach to search for low-frequency solar oscillations we have examined frequency-*amplitude* spectra.

In Section 4 we give a brief introduction to Bayesian statistics and describe how they can be used to search for low-frequency oscillations in solar data. Bayesian statistics can be used to determine the ‘posterior probability’ that a hypothesis, such as H0, is true given a set of observed data. The derivation of the posterior probability is based on the assumption that the background noise has a  $\chi^2$ , 2 degrees of freedom (d.o.f.) distribution, which is true in frequency-power spectra. Therefore, when using a Bayesian

approach to search for low-frequency solar oscillations we have examined frequency-*power* spectra. In Section 5 we discuss one component of the Bayesian calculations: the prior probability. In particular we determine whether this probability can make use of a priori knowledge to guide searches for solar oscillations. To date Bayesian statistics have only been used to search individual data sets for evidence of oscillations. We have used a Bayesian approach to derive the posterior probability that a coincident prominent feature will be detected in data observed by different instruments (Section 6).

We have searched three sets of data for evidence of low-frequency oscillations using both frequentist and Bayesian approaches. The data were observed by the Birmingham Solar Oscillations Network (BiSON), and the GOLF and Michelson Doppler Imager (MDI) instruments onboard the *SOHO* spacecraft. The results of searching the data are described in Section 7. A comparison of the results of the two different approaches is made in Section 8.

## 2 A GENERAL COMPARISON BETWEEN FREQUENTIST AND BAYESIAN STATISTICS

When using a frequentist approach to search for low-frequency solar oscillations the probability of observing, by chance, a prominent feature in a range of  $N$  frequency bins in a frequency-amplitude/power spectrum is often determined. The determined probability is dependent on the value of  $N$ , which must be chosen carefully and the choice of  $N$  is discussed in more detail in Section 3.

When adopting a frequentist approach to statistics it is common to set, a priori, an arbitrary probability detection threshold level, for example, at 1 per cent. If the probability of observing a prominent feature is less than this threshold probability the feature is considered as a mode candidate. However, the meaning of the threshold probability is commonly misunderstood. Take, for example, the frequentist approach that was used here. We determined the probability of observing a prominent spike in a frequency-amplitude spectrum by chance, if the H0 hypothesis is true. The H0 hypothesis assumes that the data being examined contain only noise. However, the determined probability, or *P* value, is commonly misinterpreted as the probability that the H0 hypothesis itself is true. In fact, we can say nothing about the validity of the hypothesis.

The problem occurs because of the non-repeatability of the experiment: we only have one Sun to observe. A similar problem has been identified in medical statistics (e.g. Berger & Sellke 1987; Sellke et al. 2001), where it has been shown that the probability that the H0 hypothesis is correct is significantly larger than the *P* value quoted in a frequentist approach. Consequently, great care must be taken when drawing conclusions from frequentist statistics. It must be made clear the frequentist threshold probability gives the chances of the data being observed if the underlying hypothesis is true and gives no information on the validity of the hypothesis itself.

To determine the probability that a given hypothesis is true we must turn to Bayesian statistics. Bayesian statistics allow us to use a priori information in a statistically rigorous manner to compare the chances that, given the observed data, different hypotheses are true. For example, here we have used Bayesian statistics to determine which of the H0 and H1 hypotheses are most likely, where the H1 hypothesis assumes there is a signal in the data. It is important to point out that we are still not determining the probability that a detection is a solar mode of oscillation as the H1 hypothesis does not specify the source of the signal. Any observed signal could con-

ceivably be some sort of structured noise. However, the Bayesian approach still gives probabilities that are less open to misinterpretation than the frequentist approach. Furthermore, significance estimates are much more conservative than those obtained with frequentist methods and so should lead to fewer false detections.

### 3 SEARCHING CONTEMPORANEOUS DATA USING FREQUENTIST STATISTICAL TECHNIQUES

The signal from solar oscillations will be common to contemporaneous data observed by different instruments. It is, therefore, pertinent to search frequency-amplitude spectra, constructed from contemporaneous data, for statistically significant, prominent concentrations of power, which lie significantly above the local noise background and that are coincident in frequency in different data sets. In Section 7 we show the results obtained when contemporaneous BiSON, GOLF and MDI data were searched.

It is possible to determine the probability of observing, by chance, prominent features that are coincident in frequency in two frequency-amplitude spectra. Proper account must be taken of any noise that is common to the two sets of data since the presence of common noise increases the probability of observing a coincident prominent noise feature. When BiSON data are compared with GOLF or MDI data any common noise is solar in origin and, more specifically, is due to solar granulation. When GOLF and MDI data are compared some of the common noise may also be instrumental as both are onboard the SOHO spacecraft. The presence of common noise means that the probability of observing coincident prominent features by chance is non-trivial to derive. A derivation of the joint probability,  $p$ , of the occurrence of coincident prominent features in two frequency-amplitude spectra is given in Broomhall et al. (2007). In order to make this derivation it was assumed that the background is slowly varying in frequency with no sharp features and that the real and imaginary noise in the frequency-amplitude spectrum has a Gaussian distribution, as is observed.

The probability of observing, by chance, a coincident, prominent feature at least once over a region of  $N$  bins in two frequency-amplitude spectra is

$$P = 1 - (1 - p)^N, \quad (1)$$

where again we recall that  $p$  is the joint probability for finding a coincident feature in a single bin. A low value of  $P$  indicates that a feature is statistically prominent compared to the background noise and, as such, is worth consideration as a ‘mode candidate’. It is important to remember that this is fundamentally different from determining the probability that a detection is a mode.

When determining the significance of any observed prominent features the value of  $N$  in equation (1) must be fixed. As  $N$  increases, the probability of detecting a prominent feature by chance in a single set of  $N$  bins increases and therefore the size of  $N$  must be suitably capped. However, as  $N$  decreases the total number of strips containing  $N$  bins in the frequency range of the frequency-amplitude spectrum that is searched increases. Consequently, the probability that at least one of these  $N$  bin ranges contains a false detection also increases and so  $N$  should not be too small. When deciding on the optimum value of  $N$  a balance between these two requirements must be sought. In the results that follow  $N$  was taken to be the number of bins in  $100 \mu\text{Hz}$ .

Various statistical tests are described in Chaplin et al. (2002) that determine the probability of observing prominent structures in a single frequency-power spectrum. These tests can be easily adapted

so they can be used to compare two frequency-amplitude spectra if the probability of observing a single prominent spike at the same frequency in each of the frequency-amplitude spectra can be calculated (Broomhall et al. 2007). These tests were originally designed to detect  $p$  modes, however, the underlying theory is still applicable when searching for  $g$  modes. An outline of the statistical tests that were applied here will now be given.

We define a spike as a single bin with a prominent amplitude in a frequency-amplitude spectrum. A ‘pair of spikes’ is then a prominent spike that occurs in the same frequency bin in each of two frequency-amplitude spectra. The simplest test that was used to compare the BiSON, GOLF and MDI data searched for individual prominent pairs of spikes. This test makes no a priori assumptions regarding the properties of the modes. Additional tests have also been formulated which do take advantage of known mode properties that are observed in frequency-power/amplitude spectra.

One such test searches for a cluster of prominent spikes. For example, we have searched for three coincident prominent spikes over a range of six bins. This test is designed to take advantage of the fact that solar oscillations are damped and the power of a mode may be spread across more than one frequency bin. The observed width of a mode is dependent on the mode’s lifetime and the length of the respective data set. Although the lifetimes of low-frequency  $p$  modes are uncertain, evidence from higher-frequency  $p$  modes implies that in a time series of length 8.5 yrs, which is the length of the data series analysed here, even very low-frequency  $p$  modes could have resolved widths (Broomhall et al. 2008). The lifetimes of  $g$  modes are less predictable and so it is uncertain whether or not the width of  $g$  modes will be resolved. Even if a mode’s lifetime is greater than the length of the time series it is still possible for its power to be spread across more than one bin for the following reason. If the mode signal is not commensurate with the window function of the observations, its maximum amplitude will be diminished and the majority of its amplitude will be divided between two consecutive frequency bins. With this in mind, a statistical test was also derived that searched for two consecutive prominent pairs of spikes.

Another statistical test that was used to search the BiSON, GOLF and MDI data looked for prominent structures whose patterns mimic those expected from the rotational splitting. In Sun-as-a-star data only mode components where  $l + m$  is even are visible and so the statistical test searched for components whose azimuthal orders,  $m$ , were separated by 2. This test assumed a separation in frequency between adjacent  $m$  components of  $0.4 \pm 0.1 \mu\text{Hz}$ . The error of  $\pm 0.1 \mu\text{Hz}$  is included to allow for the influence of magnetic fields, which shift the observed frequencies of the modes. García et al. (2004) found that the splittings of  $p$  modes can vary between  $0.38$  and  $0.45 \mu\text{Hz}$ , both of which are within the range of splittings allowed here i.e.  $0.4 \pm 0.1 \mu\text{Hz}$ .

We use a splitting of  $0.4 \pm 0.1 \mu\text{Hz}$  to maintain consistency with previous works (Chaplin et al. 2002; Broomhall et al. 2007). However, it should be noted that since the rotation in the core is not well known this value may not represent the synodic splitting of  $g$  modes. For example, García et al. (2007) suggest that the core may be rotating between 3 and 5 times faster than the radiative zone. We note here that one could question the how appropriate it is to use this test with a frequentist approach since we are using a priori knowledge. Therefore, although the results of the multiplet test are included here for completeness and consistency with previous works (Chaplin et al. 2002; Broomhall et al. 2007) we regard the results with suspicion.

More detailed descriptions of the statistical tests can be found in

Chaplin et al. (2002) and Broomhall et al. (2007). We now describe how Bayesian statistics can be used to assess the significance of any mode candidates.

#### 4 USING BAYESIAN STATISTICS TO SEARCH FOR SOLAR OSCILLATIONS

Appourchaux (2008) describes how Bayesian statistics can be used to determine the frequencies of modes in solar data and Appourchaux et al. (2009) uses Bayesian statistics to search asteroseismic data observed by the CoRoT spacecraft for evidence of oscillations. We now summarize the methods used by Appourchaux et al. (2009) and adapt them so that they can be used to search contemporaneous solar data.

Bayes theorem can be used to determine the ‘posterior probability’,  $p(H_0|x)$ , that the  $H_0$  hypothesis is true given the observed data,  $x$ . Appourchaux et al. (2009) shows that the posterior probability is given by

$$p(H_0|x) = \left[ 1 + \frac{(1-p_0)}{p_0} \frac{p(x|H_1)}{p(x|H_0)} \right]^{-1}, \quad (2)$$

where  $p_0$  is the prior probability, which is defined as the subjective probability, before any observations have been made, that  $H_0$  is true. The  $H_0$  hypothesis assumes that the data contains only noise. Therefore, in equation (2),  $p(x|H_0)$  is the probability that a spike with a power  $x$  is observed in a frequency-power spectrum that contains only noise. Similarly,  $p(x|H_1)$  is the probability that a spike with a power,  $x$ , is observed if the  $H_1$  hypothesis is true. Here, the  $H_1$  hypothesis assumes that there is a signal in the data with a maximum power spectral density per unit bin,  $H$ . We are assuming that  $H_0$  and  $H_1$  cover all possibilities. In other words there is no third hypothesis,  $H_2$  say, that is true. Appourchaux et al. (2009) derives the expressions for  $p(x|H_0)$  and  $p(x|H_1)$  that can be used to search frequency-power spectra. We now quote these expressions for reference.

We define a spike as the power spectral density contained in a single bin of the frequency-power spectrum. Frequency-power spectra have a  $\chi^2$ , 2 d.o.f. distribution and so the probability of observing a spike with a power spectral density of  $x$  if the data contain noise only is given by

$$p(x|H_0) = e^{-x}, \quad (3)$$

where we have taken the mean power spectral density of the spectrum to be 1. For the alternative  $H_1$  hypothesis we assume that the spike contains the signal from a mode which has been stochastically excited, as is the case for solar oscillations. However, as we do not know the power of the mode we assume, a priori, that the maximum power spectral density per unit bin of the mode in a frequency-power spectrum is distributed uniformly between 0 and  $H$ . The probability of observing a spike with a power spectral density,  $x$ , is then given by

$$p(x|H_1) = \frac{1}{H} \int_0^H \frac{1}{1+H'} e^{-x/(1+H')} dH'. \quad (4)$$

Equations (3) and (4) can be substituted into equation (2) to give the posterior probability.

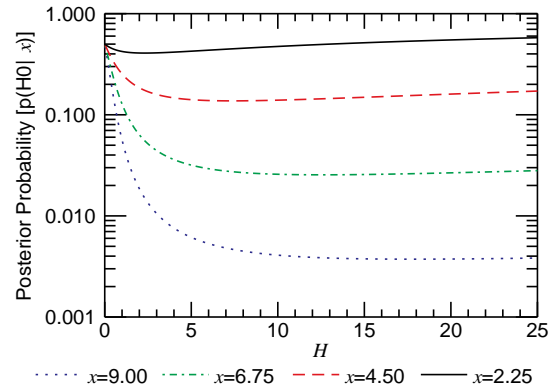


**Figure 1.** The variation of the posterior probability with the maximum power,  $H$ , for different threshold powers,  $x$ .

#### 4.1 Range of heights

In order to calculate  $p(x|H_1)$  we have to make assumptions about the maximum power spectral density per unit bin of a mode profile,  $H$ , with a frequency,  $\nu$ . Fig. 1 shows the variation with  $H$  of the posterior probability, which is related to  $p(x|H_1)$  by equation (2), for power spectral densities,  $x$ . The choice of  $H$  is most influential at low  $H$  and high  $x$  and so it is important to choose the value of  $H$  carefully to enable the significance of any prominent feature to be accurately assessed. As we are searching for oscillations that have not yet been observed we need to use models to estimate the value of  $H$ .

Notice that for each  $x$  plotted in Fig. 1 a minimum posterior probability is observed. Such minima can be understood as a manifestation of the fact that the prior on  $H$  being large is contradicted by the low power spectral density level reached by the peak (Appourchaux et al. 2009). In other words, if the mode power spectral densities were truly so high the observed peak would also be prominent.

Before we discuss the values used to constrain  $H$  it is important to define exactly what we mean by the maximum power spectral density per unit bin of a mode. In this paper we define the maximum power spectral density as the peak height of a mode’s profile in a frequency-power spectrum. Solar oscillations are damped and, if the lifetime of a mode is significantly shorter than the length of the observations, the mode will appear in a frequency-power spectrum in the form of a Lorentzian. The width of the Lorentzian,  $\Delta$ , is related to a mode’s lifetime,  $\tau$ , by the following equation:

$$\Delta = \frac{1}{\pi\tau}. \quad (5)$$

The maximum power spectral density per unit bin (or height) can be described by the following equation (Fletcher et al. 2006):

$$H = \frac{2V^2}{\pi T \Delta + 2}. \quad (6)$$

where  $V^2$  is the total power of the mode,  $T$  is the length of the time series and  $\Delta$  is in units of frequency. Consequently,  $T\Delta$  gives the width of the Lorentzian in units of bins.

For  $p$  modes the value of  $H$  was estimated in two different ways, each of which will now be described. Broomhall et al. (2008) extrapolated to low frequencies the total mode powers,  $V^2$ , and widths,  $\Delta$ , of well-defined, higher-frequency modes, whose profiles in a frequency-power spectrum can be fitted accurately. The total power,  $V^2$ , was extrapolated in preference to  $H$  as it is not

dependent on  $\Delta$ . Broomhall et al. did this in two different ways and here we have used the method that produced the largest  $H$  values.

Even so, it is possible that this method under-estimates the power of the signal from a mode. For example, Broomhall et al. (2008) found that the  $l = 0$ ,  $n = 6$  mode at  $\sim 972 \mu\text{Hz}$  is excited to a larger power than is expected from the extrapolations. In fact, the simulations performed by Broomhall et al. indicated that, if the actual power was equal to the value given by the extrapolation, the probability that the  $l = 0$ ,  $n = 6$  mode would be excited to the observed power is approximately 0.01. Furthermore, because solar oscillations are excited stochastically, the total power of a mode,  $V^2$ , varies with time. If the value of the power given by the extrapolation is regarded as a mean, the observed power of a mode is equally likely to be greater than this value as it is to be lower. Consequently, by integrating over the range 0 to  $H$  we could be underestimating the true height of the mode. More realistic probabilities may be obtained if we overestimate the range of heights over which the integration in equation (4) is made. Therefore, we have also performed a search where the maximum power spectral density per unit bin,  $H$ , was assumed to be constant at all frequencies and to have the height predicted by Broomhall et al. (2008) for a mode with a frequency of  $1500 \mu\text{Hz}$ . A larger value of  $H$  should allow signals to be detected more easily as when  $H$  tends to 0,  $p(x|H1)$  tends to  $p(x|H0)$  and so it is very difficult to determine which hypothesis is most likely to be correct (see Fig. 1).

As for low-frequency p modes we are reliant on models to predict the powers of g modes. Two groups have produced predictions of g-mode powers. The first group uses the Cambridge stochastic excitation model, as applicable to g modes (Houdek et al. 1999). The second group (Belkacem et al. 2009) uses a similar model with a different temporal-correlation between the modes and the turbulent eddies: Belkacem et al. take the eddy-time correlation function to be a Lorentzian, while Houdek et al. assume that the eddy-time correlation is a Gaussian. The authors of both papers feel that their respective models are only applicable to limited ranges in frequency and these ranges do not coincide. However, the work of Belkacem et al. predicts significantly larger g-mode powers than those predicted by Houdek et al.. Therefore, we have taken the upper limit for  $H$  to be the maximum power predicted by the work of Belkacem et al. (2009) as the larger the mode powers the more likely we are to be able to detect any oscillations. We have taken the total power,  $V^2$ , to be the constant value of  $9 \text{mm}^2 \text{s}^{-2}$  at all frequencies in the range  $(50 - 350) \mu\text{Hz}$ . We have then assumed that the lifetime of the g modes is significantly longer than the length of the observations and so all of the modes power will be confined to a single bin. Therefore the height of the mode,  $H$ , is equal to the total power,  $V^2$  i.e.  $H = 9 \text{mm}^2 \text{s}^{-2} \text{bin}^{-1}$ . Belkacem et al. (2009) note that, given the uncertainties in their model, this maximum power could, potentially, be a factor of four larger. Therefore, we have also determined the posterior probability given the observed prominent features when the maximum height,  $H$ , was  $36 \text{mm}^2 \text{s}^{-2} \text{bin}^{-1}$ .

## 4.2 Searching a range of frequencies

The statistics described above can be used to search individual bins of a frequency-power spectrum. However, there are  $\sim 400,000$  bins in the total range of frequencies searched here ( $50 - 1500 \mu\text{Hz}$ ). Consequently the chances of making a false detection are significant when searching each bin individually. We therefore consider a range of frequencies containing  $M$  bins. In the manner described by Sturrock (2008) we define the following null and alternative hypotheses:

H00: The principal peak in  $M$  bins is due to noise,

H11: The principal peak is due to an oscillatory signal with a frequency,  $\nu$ .

Then

$$P(x|H00) = 1 - [1 - P(x|H0)]^M \approx MP(x|H0), \quad (7)$$

when  $P(x|H0)$  is small. We assume only one frequency bin out of the  $M$  of interest contains a signal and so

$$P(x|H11) = P(x|H1). \quad (8)$$

Therefore,

$$\begin{aligned} p(H00|x) &= \left[ 1 + \frac{(1-p_0)}{p_0} \frac{p(x|H11)}{p(x|H00)} \right]^{-1} \\ &= \left[ 1 + \frac{(1-p_0)}{p_0} \frac{p(x|H1)}{Mp(x|H0)} \right]^{-1}. \end{aligned} \quad (9)$$

To ensure that only one mode component is present in the  $M$  bins we have taken  $M$  to be the number of bins in  $0.4 \mu\text{Hz} = 106$ , as this is the expected splitting between adjacent  $m$  components. Note that we have erred on the side of caution when setting this value of  $M$  as in Sun-as-a-star data only  $(l+m)$ -even components can be detected. Therefore, the average splitting between adjacent visible components is closer to  $0.8 \mu\text{Hz}$ . We have assumed that the components of g modes are also rotationally split by  $0.4 \mu\text{Hz}$ . It should be noted that the core rotation rate is very uncertain and so this assumption may not be valid. For example, García et al. (2007) suggest that the core might be rotating between three and five times faster than the radiative zone. However, even if this is the case there will still be only one component present in the  $M = 106$  bins under consideration. One possible extension to this work would be to test the data taking into account a faster core rotation rate.

## 4.3 Searching smoothed spectra using Bayesian techniques

The lifetimes of p modes are expected to be short enough for their profiles to have a resolved width in the frequency-power spectrum examined here. Until now we have assumed that g modes have very long lifetimes but this is not necessarily correct. García et al. (2007) have found a very interesting peak in a periodogram of a periodogram of GOLF data. They claim that this peak is due to the superposition of g modes that lie in the asymptotic range where the separation in period is approximately constant ( $\sim 24$  min). The peak is positioned close to the period predicted by standard solar models. García et al. use artificial data to show that, if this peak is evidence of g modes, the modes might have widths in a frequency-power spectrum that are commensurate with damping times of several months. However, this is not the only explanation for the observed mode widths. The observed results could also be due to an internal magnetic splitting, changes with time of the cavities in which the oscillations were trapped or a noise effect in the GOLF data. If the damping times are of the order of months and given that the data searched here are 3071 d in length, the width of these modes will be resolved in frequency-power spectra.

Appourchaux et al. (2009) describe how Bayesian statistics can be used to search for modes with resolved widths. This is done by summing the frequency-power spectrum over a given number of bins. Smoothing a spectrum alters the underlying statistics of the noise and so it is necessary to derive new equations for  $p(x|H0)$  and  $p(x|H1)$ . If we smooth a frequency-power spectrum over  $R$  bins

the underlying statistics of the noise becomes  $\chi^2$  with  $2R$  d.o.f.. We have used the equations for  $p(x|H0)$  and  $p(x|H1)$ , which are described in Section 3.2 of Appourchaux et al. (2009), to search solar data for modes with lifetimes that are shorter than the length of the time series. We now give the equations for reference.

The probability that, in a spectrum that has been smoothed over  $R$  bins, a spike with a power spectral density of  $x$  is observed if the  $H0$  hypothesis is true is given by

$$p(x|H0) = \frac{x^{R-1} e^{-x}}{\Gamma(R)}, \quad (10)$$

where  $\Gamma(R)$  is the gamma function and we have assumed that the mean of the unsmoothed frequency-power spectrum is unity. For the alternative hypothesis we again assume that the spike contains the signal from a stochastically excited mode. However, when dealing with smoothed spectra, instead of making assumptions about  $H$  we must make assumptions about the total mode power,  $V^2$ , and the mode linewidth,  $\Delta$ . Here we assumed, a priori, that the mode amplitude is distributed uniformly between 0 and  $V$  and that the mode linewidth is distributed uniformly between 0 and  $\Delta$ . Then the probability of observing a spike with a power spectral density  $x$  in a smoothed spectrum, if the  $H1$  hypothesis is true, is given by

$$p(x|H1) = \frac{1}{V\Delta} \int_0^V \int_0^\Delta \frac{\lambda^\nu}{\Gamma(\nu)} x^{\nu-1} e^{-\lambda x} dV' d\Delta', \quad (11)$$

where  $\lambda$  and  $\nu$  are given in Appourchaux (2004) and are related to the line profile of the mode, i.e. they are related to  $V$  and  $\Delta$ . Equations (10) and (11) can be substituted into equation (9) to give the posterior probability.

When searching for p modes, we have used the values for  $V^2$  and  $\Delta$  extrapolated by Broomhall et al. (2008) as the upper limits on the mode powers and lifetimes. When searching for g modes we took  $V^2$  to be both  $9 \text{ mm}^2 \text{ s}^2$  and  $36 \text{ mm}^2 \text{ s}^2$  (see Section 4.1 for details). As the lifetimes of the g modes are not known we used a range of different values: 1, 2, 3, and 4 months. Equation (9) was then used to determine the posterior probability. The posterior probability, given by Equation (9), is also dependent on the prior probability,  $p_0$ , and we now discuss the value given to  $p_0$ .

## 5 WHAT VALUE SHOULD THE PRIOR PROBABILITY TAKE?

One important question when applying Bayesian statistics is what value should the prior probability,  $p_0$ , take? We define  $p_0$  as the subjective probability that the  $H0$  hypothesis is correct, as assigned before the data are examined. If  $p_0$  is set at a very high (or very low) value any statistical tests are likely to just confirm the initial belief that  $H0$  (or  $H1$ ) is correct. Therefore, it is common to set  $p_0 = 0.5$  so as to avoid prejudicing one hypothesis over the other. However, we know that low-frequency p modes have narrow widths, which cover at most a few bins only. In which case, would we expect the probability that  $H1$  and  $H0$  are true to be the same at all frequencies? Is it possible to use our knowledge of the solar structure to tell us which hypothesis is more likely to be true at a given frequency? Can we also use this knowledge to then systematically guide the regions in frequency we wish to search?

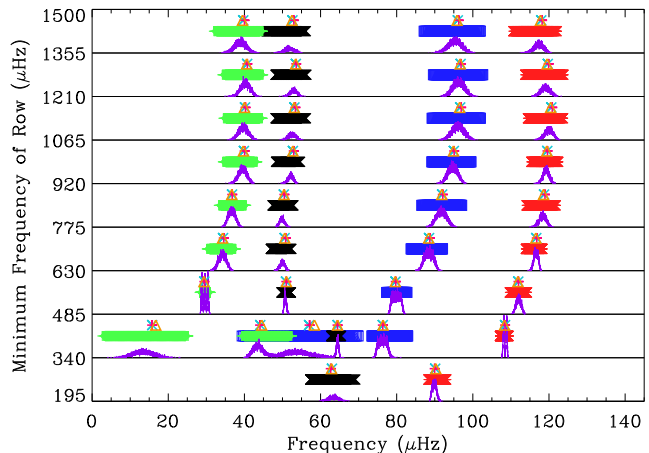


**Figure 2.** An echelle diagram showing the frequencies predicted by different solar models. At the centre of each row, the black symbols represent the frequencies of the  $l = 0$  modes, the red symbols represent the  $l = 1$  modes, the green symbols represent the  $l = 2$  modes and the blue symbols represent the  $l = 3$  modes. All components with  $l+m$  even have been plotted assuming a symmetric synodic splitting of  $0.4 \mu\text{Hz}$ . The purple curve shows the frequency distribution of the models. Towards the top of each row the  $m = 0$  components of the Saclay seismic model frequencies (Turck-Chièze et al. 2001, blue crosses), the M1 model (Zaatri et al. 2007, orange triangles) and Model S frequencies (Christensen-Dalsgaard & Berthomieu 1991, pink plus signs) are shown for comparison purposes.

### 5.1 A non-uniform prior that can be used to search for p modes

We have looked at the p-mode frequencies predicted by 5000 solar models (see Bahcall, Serenelli & Basu 2006; Chaplin et al. 2007, for details), whose input parameters, such as composition and age, have been altered within their error bars. The frequencies of the modes predicted by the models have been plotted on an echelle diagram in Fig. 2. Different colours have been used to represent the different  $l$  and the predicted frequencies of all of the visible components (when  $l+m$  is even) are plotted. We have taken the synodic splitting to be  $0.4 \mu\text{Hz}$  and symmetric, which is a reasonable assumption for the frequency range of interest here ( $< 1500 \mu\text{Hz}$ , Chaplin et al. 2002). Although the rotation rate of the solar core is uncertain this assumption remains valid as the p mode rotational splitting is relatively insensitive to the rotation speed of the core (see e.g. García et al. 2008). For reference the centroid frequencies predicted by the Saclay seismic model (Turck-Chièze et al. 2001), the M1 model (Zaatri et al. 2007), and Model S (Christensen-Dalsgaard & Berthomieu 1991) have been included. The purple curve in Fig. 2 shows the shape of the distribution of the model frequencies.

The frequencies predicted by the models for each individual mode are spread over a reasonably large range, indicating the uncertainties associated with solar modelling. However, there are definite gaps in frequency where none of the models predict a mode should be detected. Solar models would have to be changed beyond reasonable expectations to account for any mode frequencies that lie outside the predicted ranges. In the frequency ranges where no modes are expected, we can set the prior probability that  $H0$  is true to unity thereby making it impossible for a prominent feature, which is likely to be noise, to pass any statistical tests. We have, therefore, defined an inverted top-hat prior that is equal to 0.5 in the frequency ranges where, according to the models, the modes

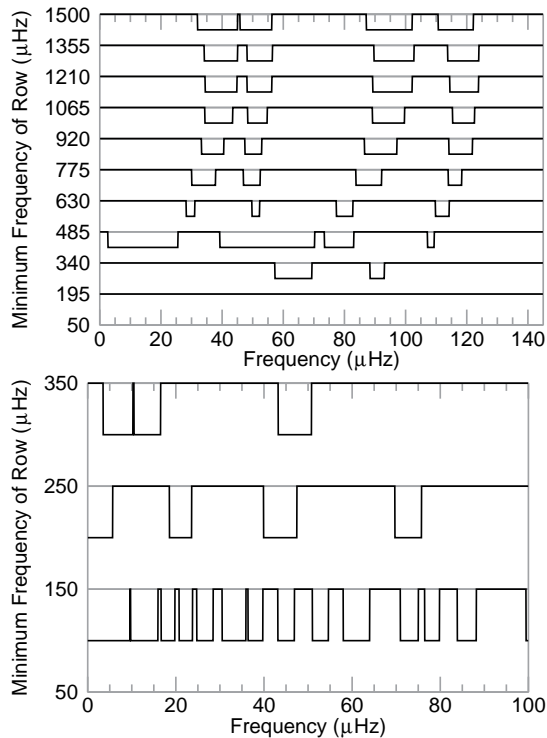


**Figure 3.** Top panel: An echelle diagram showing the variation of the prior probability with frequency for p modes. Bottom panel: An echelle diagram showing the variation of the prior probability for g modes. In each panel the prior probability was either 1.0, at frequencies where modes are not expected to be observed, or 0.5 at frequencies where modes are expected.

should be observed and  $p_0 = 1$  at all other frequencies. Such a prior is shown in the top panel of Fig. 3. This approach should severely limit the number of false detections that are made.

## 5.2 A non-uniform prior that can be used to search for g modes

The sensitivity of g-mode frequency predictions to solar models is of the order of 1% (Appourchaux et al. 2010). This means, for example, that at  $100 \mu\text{Hz}$  the expected error on the predicted mode frequencies is  $1 \mu\text{Hz}$ . We have used this error estimate to produce two inverted top-hat prior distributions for g modes. For the first prior the centres of each hat are determined by the mode frequencies predicted by the M1 model (Zaatri et al. 2007) and the width of each hat was 2 per cent of the mode frequency i.e.  $\pm 1$  per cent. For the second prior, the width of each hat was still 2 per cent of the mode frequency, however, we have used the frequencies predicted by the Saclay solar model (Mathur et al. 2007). Frequencies where modes are expected to be observed have been given a prior probability that the  $H_0$  hypothesis is true of 0.5 and elsewhere the prior is unity. The bottom panel of Fig. 3 shows the M1 model prior distribution, where all visible components in Sun-as-a-star data (when  $l + m$  is even) have been plotted for  $l = 1$  and  $l = 2$  modes. We have not plotted the Saclay model prior here as it is very similar to the M1 model prior. We have assumed that the different  $m$  components are still separated by  $0.4 \mu\text{Hz}$ . As previously mentioned, the results of García et al. (2007) imply that this assumption may not be valid for g modes. In the absence of a definitive estimate for g-mode splittings, we have chosen to maintain consistency with the splitting

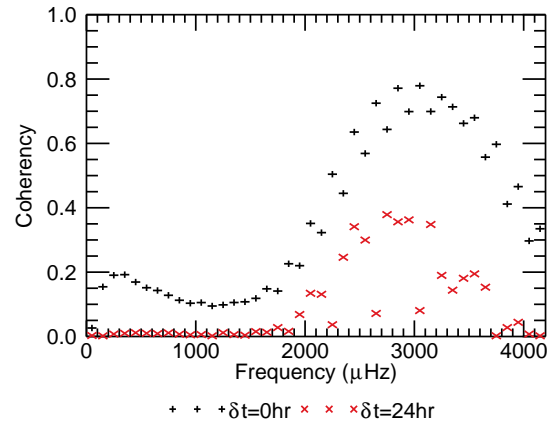


**Figure 4.** The coherency observed between BiSON and GOLF data when the GOLF data starts 24 h after the BiSON data.

value used when searching for p modes. However, as new information on the rotational splitting of g modes becomes available an updated uneven prior probability should be constructed. Notice that despite the large number of g modes that are present at low frequencies the prior is not uniform with frequency and so, again, this approach should limit the number of type I false detections. It is possible that an improved g-mode uneven prior probability could be constructed by producing models for g modes that are similar to those used to construct the p-mode uneven prior probability.

## 6 SEARCHING MORE THAN ONE DATA SET USING BAYESIAN STATISTICS

As mentioned in Section 3, Broomhall et al. (2007) developed the statistics necessary to allow two sets of contemporaneous data to be compared using a frequentist approach. This has been done both to lower the amplitude/power threshold levels and to improve the reliability of any detection because if a prominent feature is found in data observed by two different instruments it is more likely to be solar in origin (although it should be noted that there may be some consistent spacecraft signatures in the GOLF and MDI data). However, it is worth mentioning that by comparing the data we are limited by the signal-to-noise ratios of the worst instrument. For example, there is a known instability problem with the MDI instrument that causes low-frequency noise. Consequently, some mode candidates that are only prominent in one data set have not been highlighted here. This could increase the number of type II errors but, conversely, will limit the number of type I errors, which we consider to be more serious than type II errors. In this paper, we aim to use Bayesian statistics to compare multiple data sets. Since contemporaneous BiSON, GOLF and MDI data will contain some common noise (see Fig. 4), the probability that a prominent spike, which is found in the same frequency bin in each frequency-power spectrum, is due to noise is non-trivial to derive, whether using a frequentist or Bayesian approach. We offer a solution that avoids the need to consider the effect on the statistics of the noise shared by each data set.

Fig. 4 shows the coherency (Elsworth et al. 1994) of the BiSON and GOLF data when the GOLF time series begins 24 h after the BiSON data. The separation in start times means that the coherency of the noise observed between the data is reduced to zero below  $1500 \mu\text{Hz}$  and the same is true for the other combinations of the BiSON, GOLF and MDI data. Therefore, separating the start times

of the data sets removes the complication caused by the common noise. When no common noise is shared by the two data sets under consideration the posterior probability,  $p(\text{H00}|x)$ , that, if a feature appears in both frequency-power spectra, H00 is correct, is given by

$$p(\text{H00}|x) = \left[ 1 + \frac{(1-p_0)}{p_0} \frac{p(x_1|\text{H1})p(x_2|\text{H1})}{M p(x_1|\text{H0})p(x_2|\text{H0})} \right]^{-1}, \quad (12)$$

where  $x_1$  is the power spectral density of a spike in the first frequency-power spectrum and  $x_2$  is the power spectral density of a spike at exactly the same frequency in the second frequency-power spectrum. When comparing two sets of non-contemporaneous data for coincident prominent features we are assuming that the mode signatures will still be coherent if we shift the start times and we now show that this assumption is valid at low frequencies.

### 6.1 The coherency of modes in shifted spectra

Simulations were performed to investigate how a modes' coherency changes in non-contemporaneous data. The modes were simulated by creating a damped oscillator that was re-excited randomly in time (Chaplin et al. 1997). The power and damping time of each mode were determined by fitting the BiSON data using a standard likelihood maximization method (e.g. Chaplin et al. 1999). Simulations were performed for  $l = 1$  modes with  $10 \leq n \leq 22$  and a separate simulation was performed for each mode. These modes are at higher frequencies than the ones we are searching for in this paper. However, they have a large S/N ratio and so their properties, such as lifetime and power, can be determined more accurately. The simulations were performed using two identical time series that contained the signal from one simulated mode only.

The top panel of Fig. 5 shows the coherency (Elsworth et al. 1994) of the modes when the start times of the simulated time series were shifted so that they were separated by  $\delta t = 0$  h (black plus signs),  $\delta t = 12$  h (black crosses) and  $\delta t = 24$  h (black diamonds). The coherency of two unshifted identical sets of data is always unity, independent of the power and width of the simulated mode. The top panel of Fig. 5 shows that the effect on the coherency of a mode of separating the start times of two data sets is frequency dependent. More specifically (bottom panel of Fig. 5) the magnitude of the decrease in coherency is lifetime dependent. The coherency of a low-frequency mode, with a long lifetime, is reduced by less than the coherency of a higher-frequency mode, with a short lifetime. This is because, as the time shift represents a smaller proportion of a low-frequency modes' lifetime, the mode experiences less damping over the duration of the shift. The magnitude of the decrease in coherency increases as the length of the shift in start times increases relative to the mode lifetime. However, is the decrease in coherency observed by modes below  $1500 \mu\text{Hz}$  significant when a time shift of 24 h is introduced?

Modes with a frequency of about  $1500 \mu\text{Hz}$  have a lifetime of approximately 1 month and so 24 h is equivalent to 1/30th of the mode's lifetime. Therefore, for each of the modes plotted in Fig. 5, the start times of the two simulated time series were separated by one-thirtieth of the mode's lifetime. The triangle symbols in the top panel of Fig. 5 shows that this only decreases the coherency by a very small amount at all frequencies. Fig. 6 plots the variation in the coherency with  $\delta t/\tau$  for three  $l = 1$  modes. The values of coherency plotted in Fig. 6 were determined using the same simulated spectra as were used to produce Fig. 5. Fig. 6 shows that if  $\delta t/\tau$  is small, the coherency decreases by only a small amount. Notice that size of the decrease in coherency shows some dependence on  $n$ . However,

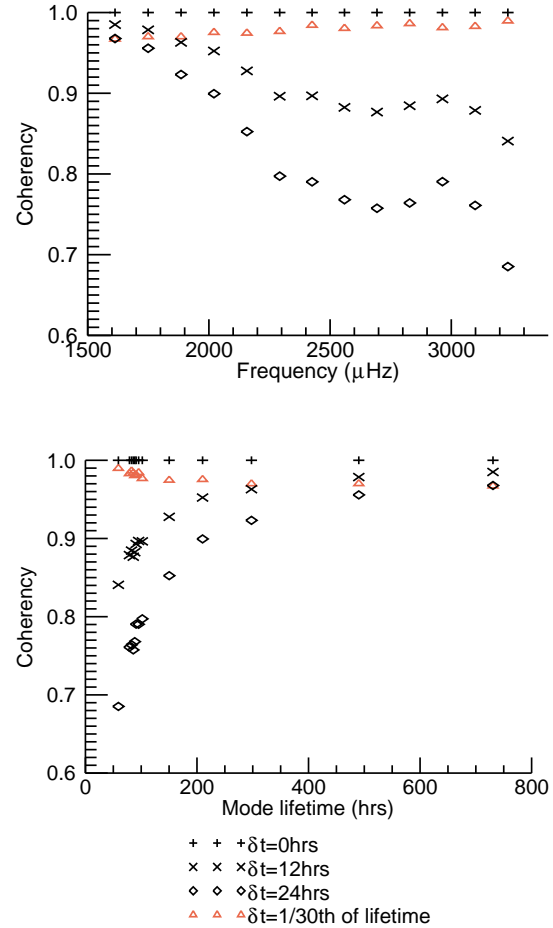


**Figure 5.** Top panel: The effect of separating the start time of time series that contain only the signal from a mode. The pairs of time series were created to contain one mode that has the same power and lifetime as is observed in  $\sim 8.5$  yrs of BiSON data. Bottom panel: The coherency plotted as a function of lifetime.

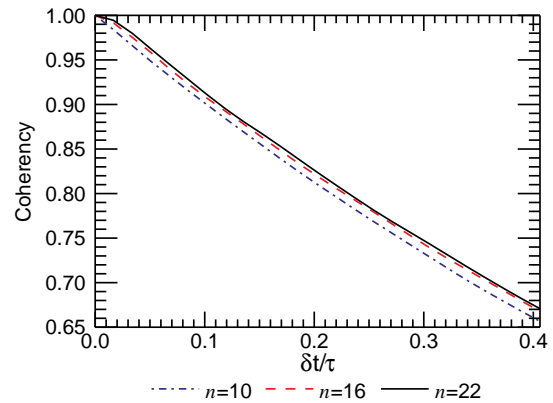


**Figure 6.** The variation in the coherency of three modes with  $\delta t/\tau$ . The results have been plotted for the  $l = 1$ ,  $n = 10$  mode, whose frequency is approximately  $1612 \mu\text{Hz}$ , the  $l = 1$ ,  $n = 16$  mode, whose frequency is approximately  $2425 \mu\text{Hz}$  and the  $l = 1$ ,  $n = 22$  mode, whose frequency is approximately  $3233 \mu\text{Hz}$ .

this dependence is small and is likely to occur because the power of the modes decreases with  $n$ . We conclude that, if the start times of two time series are separated by 24 h the low-frequency modes will still be coherent and so the data can be compared to search for low-frequency oscillations.

Note that it is possible to separate the start times of the time series by less than 24 h and still significantly reduce the amount of common noise shared by the data. However, we are dealing with long data sets and so 24 h is only a small fraction of the total observation time. Therefore a shift of 24 h was used to ensure that there was as little common noise present as possible.

A table summarizing the main assumptions made with both the frequentist and Bayesian approaches can be found in Appendix A. We now describe the results of using both the frequentist approach and Bayesian statistics to search BiSON, GOLF and MDI data.

## 7 RESULTS OF SEARCHING PAIRS OF DATA SETS FOR LOW-FREQUENCY P MODES AND G MODES

### 7.1 Observational data

In this paper we made use of contemporaneous BiSON, GOLF and MDI time series. Each data set consisted of 3071 d of Sun-as-a-star Doppler velocity observations, made between 1996 April 20 and 2004 September 15, and so the data span most of solar activity cycle 23. We have used data sets that extend only as far as 2004 to maintain consistency with Broomhall et al. (2007). The BiSON data were processed in the manner described by Appourchaux et al. (2000) and Chaplin et al. (2002). The GOLF data were processed in the manner described by García et al. (2005), and the MDI-Luminosity Oscillations Imager (LOI) proxy data were processed in the manner described by Scherrer et al. (1995). When considered individually each time series is stored on a different cadence: BiSON data are stored on a 40 s cadence, GOLF data are stored on a 20 s cadence and MDI data are stored on a 60 s cadence. Each time series was, therefore, re-binned to a common cadence of 120 s. Hence the time series contained 2211 120 samples, giving a bin width in the frequency domain of  $0.004 \mu\text{Hz}$ . It is possible that some aliasing could be present in the data due to the cut-off frequency of  $4167 \mu\text{Hz}$ . However, no aliasing was found in the frequency range searched here i.e. between 50 and  $1500 \mu\text{Hz}$ . The duty cycle of the BiSON time series was 78.6 per cent; the duty cycle of the GOLF time series was 93.4 per cent and the duty cycle of the MDI time series was 91.3 per cent.

### 7.2 Using a frequentist approach

The frequentist statistics described in Section 3 and Broomhall et al. (2007) were used to search contemporaneous BiSON, GOLF and MDI frequency-amplitude spectra for low-frequency p modes, g modes and mixed modes. Amplitude threshold levels were calculated for a 1 per cent probability of detecting a prominent feature by chance in  $100 \mu\text{Hz}$ . The spectra were searched for prominent spikes or patterns of spikes found in the same frequency bin or bins in any two of the frequency-amplitude spectra.

If the mode signal is not commensurate with the window function of the observations the maximum observed amplitude of the mode can be diminished. The ‘bin-shifting’ strategy of Chaplin et al. (2002) was therefore applied in an attempt to circumvent this problem.

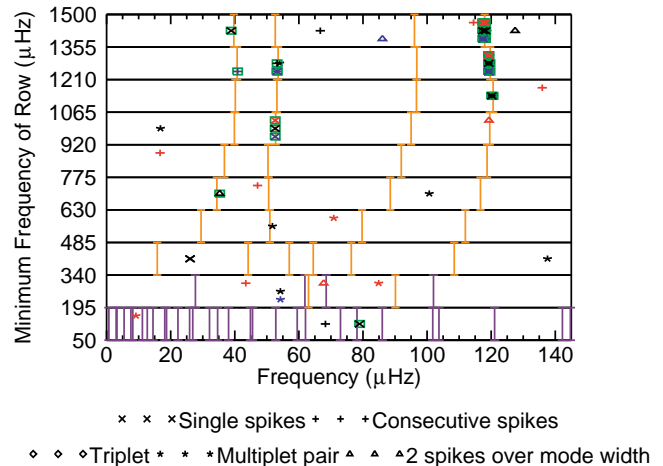


**Figure 7.** An echelle plot, modulo  $145 \mu\text{Hz}$ , marking locations in frequency of occurrences uncovered by the test searches. Locations in frequency where spikes, or patterns of spikes, were found in the same bin, or bins, in BiSON and GOLF frequency-amplitude spectra at levels sufficient to record  $P \leq 1$  per cent are marked by the black symbols in the middle of each row. A different symbol has been used for each test (see figure legend). We have also recorded prominent spikes or patterns of spikes found by comparing either the BiSON and MDI frequency-amplitude spectra (red symbols at top of each row) or the GOLF and MDI frequency-amplitude spectra (blue symbols at bottom of each row). Symbols surrounded by a green square represent the prominent occurrences listed in Table 1. The orange vertical lines mark locations of the frequencies of p modes with  $l = 0 - 3$  predicted by the Saclay seismic model (Turck-Chièze et al. 2001). The vertical purple lines mark locations of the central frequencies of g modes with  $l = 1 - 2$  predicted by the M1 model (Zaatri et al. 2007).

Fig. 7 shows visually, in the form of an echelle diagram, the locations in frequency where prominent spikes or patterns of spikes were observed. The entire range that was searched ( $50 - 1500 \mu\text{Hz}$ ) has been split into strips of  $145 \mu\text{Hz}$ . These strips have then been placed one above another. The bottom left-hand corner of the plot represents  $50 \mu\text{Hz}$  and the top right-hand corner of the plot represents  $1500 \mu\text{Hz}$ . A repeat frequency of  $145 \mu\text{Hz}$  was chosen in preference to the  $100 \mu\text{Hz}$  slice on which the searches were performed because at low frequencies consecutive overtones of the low- $l$  modes are separated in frequency by approximately this amount. At higher frequencies the spacing between modes with the same  $l$  and adjacent  $n$  is  $\sim 135 \mu\text{Hz}$ , however, this separation increases at low frequencies (low  $n$ ). The choice of repeat frequency means that the majority of the predicted p-mode frequencies are arranged in four near-vertical strips, one for each  $l$  between 0 and 3.

Artifacts, positioned in frequency at overtones of the  $11.57 \mu\text{Hz}$  diurnal frequency, may be visible in frequency-amplitude spectra because of signatures of either the window function (for the BiSON data) or the spacecraft operation (for the GOLF and MDI data). To prevent any of these artefacts being confused with mode candidates, any detections found to be closer than  $0.3 \mu\text{Hz}$  to a daily harmonic frequency were discounted. A distance of  $0.3 \mu\text{Hz}$  is sufficient to remove any false detections due to the daily harmonics as their frequencies are well defined and their peaks have a width of less than  $0.3 \mu\text{Hz}$ . The MDI data contain harmonics of  $52.125 \mu\text{Hz}$  due to beats between the spacecraft timing system and the instrument sampling rate. Any detections found when the MDI data were searched that lay within  $0.3 \mu\text{Hz}$  of these harmonic frequencies were also discounted.

Detections were only considered as possible mode candidates if

**Table 1.** Candidates found to be closer than  $1\mu\text{Hz}$  to the predicted frequencies of p modes from the Saclay seismic model and the predicted frequencies of g modes from the M1 model.  $P$  is the probability that, assuming the data contains only noise, a coincident prominent feature is observed at least once in  $100\mu\text{Hz}$ . The last column of this table indicates whether the modes were also detected using a Bayesian approach (see Sections 7.3 and 7.4).

$l$	$n$	$m$	Frequency ( $\mu\text{Hz}$ )	Probability ( $P$ )	Number of tests passed	Distance from model frequency ( $\mu\text{Hz}$ )	Detected with the Bayesian approach
1	-4	+1	$128.951 \pm 0.002$	$8.7 \times 10^{-3}$	1	$0.421^a$	n
2	3	-2	$664.515 \pm 0.002$	$6.7 \times 10^{-3}$	1		n
2	3	0	$665.284 \pm 0.002$	$6.7 \times 10^{-3}$	1	0.880	n
2	3	+2	$666.128 \pm 0.002$	$6.7 \times 10^{-3}$	1		n
0	6	0	$972.613 \pm 0.002$	$3.9 \times 10^{-5}$	1	0.132	y
1	7	-1	$1185.196 \pm 0.005$	$1.9 \times 10^{-3}$	4		y
1	7	+1	$1185.981 \pm 0.005$	$3.0 \times 10^{-3}$	1		n
		mean	$1185.589 \pm 0.004$			0.027	
2	7	0	$1250.893 \pm 0.007$	$6.3 \times 10^{-3}$	1	0.159	n
0	8	0	$1263.205 \pm 0.007$	$2.1 \times 10^{-4}$	2	0.319	y
1	8	-1	$1329.236 \pm 0.005$	$2.7 \times 10^{-11}$	4		y
1	8	+1	$1330.037 \pm 0.007$	$1.7 \times 10^{-3}$	1		y
		mean	$1329.637 \pm 0.004$			0.060	
2	8	-2	$1393.871 \pm 0.007$	$4.0 \times 10^{-4}$	1	$0.036^b$	y
1	9	-1	$1472.432 \pm 0.008$	$3.8 \times 10^{-11}$	4		y
1	9	+1	$1473.269 \pm 0.009$	$3.7 \times 10^{-8}$	4		y
		mean	$1472.851 \pm 0.006$			0.122	

<sup>a</sup>Difference with model frequency assumes  $m = \pm 1$  components lie  $\pm 0.4\mu\text{Hz}$  from central frequency.

<sup>b</sup>Difference with model frequency assumes  $m = -2$  component lies  $-0.8\mu\text{Hz}$  from the central frequency.

they were positioned within  $1\mu\text{Hz}$  of a predicted mode frequency. A maximum separation between a detection and a model frequency of  $1\mu\text{Hz}$  was allowed to account for any uncertainties in the model frequencies, any shifts due to the effects of magnetic fields, and because the power of some modes is spread across more than one frequency bin. It should be noted that Figs 2 and 3, which show the frequencies predicted by different solar models and the uneven priors used in the Bayesian approach, suggest that the allowed difference with the model should be larger than  $\pm 1\mu\text{Hz}$ . However, it was felt that an increase in the allowed difference between the model and the observed frequencies would significantly increase the number of type I false detections that were considered as mode candidates. Any detections that lie within  $1\mu\text{Hz}$  of a model frequency are surrounded by a green square in Fig. 7 and are listed in Table 1. We have compared the observed mode candidates with both the Saclay seismic model (Turck-Chièze et al. 2001; Mathur et al. 2007) and the M1 model frequencies (Zaatri et al. 2007). However, we have not plotted all of these frequencies in Fig. 7 as both models predict similar frequencies. In cases where the outer components of a rotationally split mode appear to have been uncovered, the mean of the component frequencies has been determined, in order to give an estimate of the centroid frequency of the mode. Estimates of the uncertainties in frequency were calculated in the manner described by Chaplin et al. (2002).

In the p-mode frequency range all of the listed candidates correspond to previously claimed detections (see e.g. Toutain et al. 1998; Bertello et al. 2000; García et al. 2001; Chaplin et al. 2002; Broomhall et al. 2007; Salabert et al. 2009). One of the detections in the g-mode range lies close to the predicted frequencies. To improve confidence in the detections we required that each mode

candidate passed more than one of the statistical tests, as it has been determined that this requirement significantly reduces the number of false detections made. As can be seen from Table 1 this discounts the g-mode candidate and some of the detections in the p-mode range. For comparison purposes the last column of Table 1 indicates whether the candidates were also detected when Bayesian statistics were used (see Sections 7.3 and 7.4).

Several multiplet detections lie close to the predicted mode frequencies but are not highlighted by a green square in Fig. 7. This is because not all of the detected components could be associated with the predicted frequencies of the components of one mode. For example, a triplet was detected in the BiSON and MDI data at  $\sim 1039\mu\text{Hz}$ . However, the mode closest to the detection is the  $l = 1, n = 6$  mode, which only has two visible components ( $m = \pm 1$ ). Since only two of the three detected spikes could be associated with model mode frequencies this was not counted as a mode candidate. Similarly the multiplet candidate at  $\sim 537\mu\text{Hz}$  is closest to the  $l = 0, n = 3$  mode, which cannot be observed as a multiplet (as  $l = 0$ ).

In Fig. 7 we can see that coincident multiplet detections are made at  $\sim 249\mu\text{Hz}$  in the BiSON and GOLF data and the GOLF and MDI data, which do not correspond to a predicted mode frequency. One of the detected components is at the same frequency in each detection (at  $248.474\mu\text{Hz}$ ). This component is particularly prominent in the GOLF data. The second component observed in the BiSON and GOLF data is not at the same frequency as the second component that is observed in the GOLF and MDI data. Therefore, these detections are not truly coincident.

It is apparent from Fig. 7 that the analysis has uncovered several occurrences of  $P \leq 1$  per cent that lie well away from the predicted

mode frequencies. The number of these detections exceeds the number expected ( $< 2$ ) given the range in frequencies searched, the threshold probability, and the number of statistical tests performed. This is most likely to be due to the misleading significance levels assigned when adopting a frequentist approach. It could also indicate that the statistical distribution in the noise is slightly different to the Gaussian distribution, which was assumed when deriving the statistical tests. It is also worth noting that given the large number of g modes that can theoretically be detected, particularly at very low frequencies, it is hardly surprising that some of the detections lie close to predicted mode frequencies.

### 7.2.1 Searching for g mode peaks in contemporaneous data

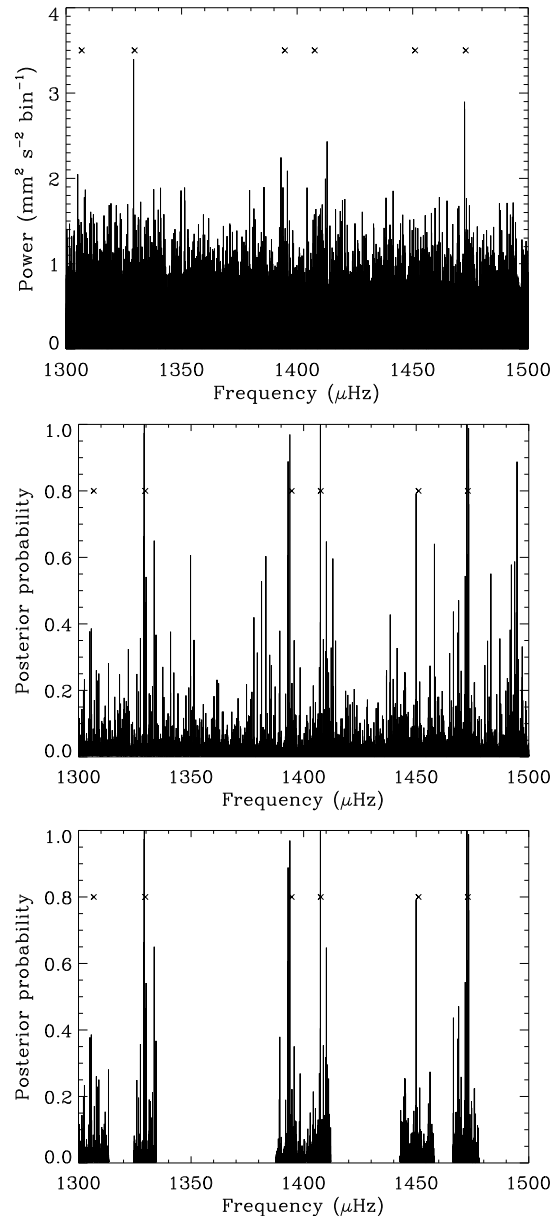
As previously mentioned the results obtained by García et al. (2007) could imply that g modes may have lifetimes of the order of months, not years. If this is true they will have a resolved width in a frequency-amplitude spectrum and so we have searched the contemporaneous, very low-frequency ( $\nu < 350 \mu\text{Hz}$ ) BiSON, GOLF and MDI data for evidence of prominent peaks with various widths. We have searched for clusters containing two, three, four and five spikes. We allow a cluster to be spread over twice the width of the mode and took the widths of the modes to be the number of bins covered if the mode lifetimes were 1, 2, 3 and 4 months, respectively. However, no statistically significant peaks were found within  $4 \mu\text{Hz}$  of the model g-mode frequencies.

### 7.3 Results of searching the data using Bayesian techniques

The statistics outlined in Sections 4-6 were used to search BiSON, GOLF and MDI data in pairs with a Bayesian approach, respectively. The start times of each pair of time series were separated by 24 h so that only a minimal amount of common noise was present in the data. The ‘bin-shifting’ strategy of Chaplin et al. (2002) was again applied. Equation (12) was used to determine the posterior probability,  $p(\text{H00}|x)$ , where initially we took the height of the p modes,  $H$ , to be given by the extrapolation described in Broomhall et al. (2008) (see Section 4.1). We have assumed that g mode lifetimes are sufficiently long for all of their power to be contained in one bin and the maximum g-mode height was taken to be  $9 \text{ mm}^2 \text{ s}^{-2} \text{ bin}^{-1}$  at all frequencies. The frequency range of  $250 - 1500 \mu\text{Hz}$  was searched for solar p modes and the frequency range of  $50 - 350 \mu\text{Hz}$  was searched for g modes.

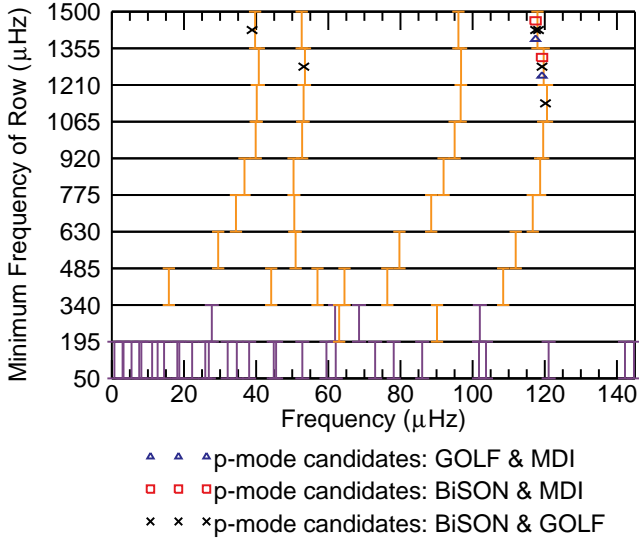
The top panel of Fig. 8 shows the BiSON spectrum over the range  $1300 \mu\text{Hz}$  to  $1500 \mu\text{Hz}$ . The crosses above the spectrum show the p-mode frequencies predicted by the Saclay seismic model (Turck-Chièze et al. 2001). As can be seen, it is difficult to distinguish possible mode candidates from the background noise. The middle panel of Fig. 8 shows  $[1 - p(\text{H00}|x)]$ , for observing a prominent feature in the BiSON and GOLF data, calculated with a uniform prior of  $p_0(\nu) = 0.5$ . As  $[1 - p(\text{H00}|x)]$  approaches unity the more likely we are to reject the H00 hypothesis that the frequency-power spectrum contains noise only. Four mode candidates are clearly visible in this plot, at  $\sim 1330 \mu\text{Hz}$ ,  $\sim 1393 \mu\text{Hz}$  and two at  $\sim 1472 \mu\text{Hz}$ . All four candidates lie close to predicted mode frequencies. The bottom panel shows the posterior probability over the same range of frequencies, only this time the top-hat prior probability described in Section 5 was used. All of the mode candidates are allowed by the uneven prior.

Fig. 9 is an echelle diagram showing the results of searching the BiSON, GOLF and MDI data using a Bayesian approach. Mode



**Figure 8.** Top panel: a section of the BiSON frequency-power spectrum. Middle panel: the posterior probability observed when BiSON and GOLF data are searched for p modes. The BiSON data was shifted to start 24 h after the GOLF data. A uniform prior probability of  $p_0 = 0.5$  was used. Bottom panel: The posterior probability observed when BiSON and GOLF data were searched for p modes. However, in this panel a the inverted top-hat prior described in Section 5 was used.

candidates have been plotted if  $p(\text{H00}|x) \leq 0.01$ . Therefore, at the plotted frequencies, we reject the H00 hypothesis that the data contains noise only, in favour of the H11 hypothesis which states that there is some signal in the data. The non-uniform prior described in Section 5 was applied and resulted in one p-mode candidate being discounted. This candidate was detected in the BiSON-MDI combination and the GOLF-MDI combination. The frequency of the candidate corresponds to a spacecraft frequency that is very prominent in the MDI frequency-power spectrum. Therefore, the fact that this candidate is discounted is a good example of how advantageous the uneven prior can be. Very few detections are made in the p-mode frequency range. However, all of the candidates that



**Figure 9.** An echelle plot, modulo  $145 \mu\text{Hz}$ , marking locations in frequency of occurrences uncovered by the Bayesian test searches. Realistic estimates of the upper limit on the modes powers were used to calculate the Bayesian probability,  $p(H0|x)$ . The different symbols represent the different pairings of data that were searched (see legend).

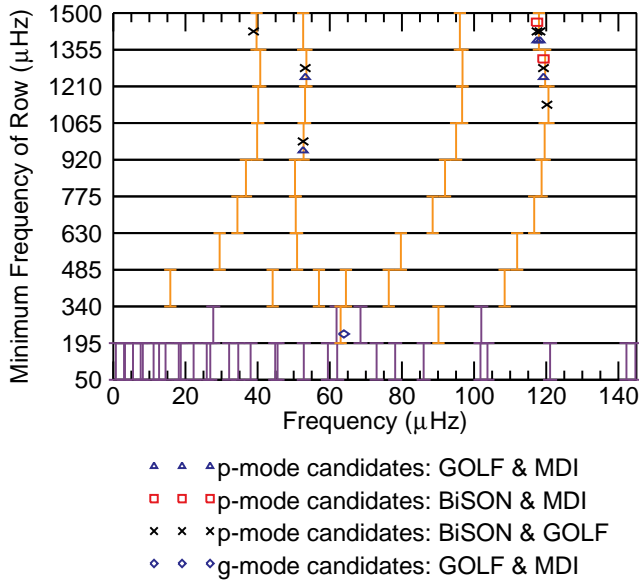


**Figure 10.** An echelle plot, modulo  $145 \mu\text{Hz}$ , marking locations in frequency of occurrences uncovered by the Bayesian test searches. The maximum power,  $H$ , was overestimated when calculating  $p(H0|x)$ . The different symbols represent the different pairings of data that were searched (see legend).

are detected correspond to mode frequencies. This implies that the Bayesian approach can successfully discriminate between signal and noise. No candidates are found in the g-mode range.

Fig. 10 is an echelle diagram that again shows the results of using Bayesian methods to search for solar oscillations. The only difference between Figs 9 and 10 is that larger maximum heights,  $H$ , have been used when determining the posterior probability. When searching for the p modes we set  $H$  to be the height a mode at  $1500 \mu\text{Hz}$  is expected to have. When searching for g modes the maximum height was taken to be  $36 \text{mm}^2 \text{s}^{-2} \text{bin}^{-1}$ , which is four

times larger than the heights assumed when producing Fig. 9 (see Section 4.1 for details). More mode candidates are detected in the p-mode range than were found when the lower heights were used (see Fig. 9). Furthermore, the  $p(H0|x)$  is lower when the larger values of  $H$  were used for all of the candidates that are plotted in both Figs 9 and 10. This could indicate that we were correct to overestimate the upper limit of  $H$  when determining  $p(x|H11)$ .

Fig. 10 shows that one g-mode candidate was detected. Even though this candidate is close to a predicted p-mode frequency ( $l = 0, n = 1$ ) it has been classified as a g-mode candidate as it was detected when the value for  $H$  was assumed to be  $36 \text{mm}^2 \text{s}^{-2} \text{bin}^{-1}$ , i.e.  $H$  was set using the g-mode models. However, we do not rule out the possibility that this detection is a p mode. A peak in this frequency region is mentioned by Turck-Chièze et al. (2004), who looked at GOLF data only.

Table 2 lists the mode candidates that are shown in Fig. 10 along with the minimum observed posterior probability,  $p(H00|x)$ . The value of  $p(H00|x)$  quoted in Table 2 is dependent on which of the two sets of data were considered. The  $l = 1, n = 9, m = -1$  mode candidate at  $1472.433 \mu\text{Hz}$  was detected at a significant level in all three combinations of data (see Fig. 10). It was most prominent in the BiSON-GOLF combination, when  $p(H00|x) = 1.6 \times 10^{-7}$ . When this candidate was observed in the GOLF-MDI combination  $p(H00|x) = 2.3 \times 10^{-5}$  and when it was observed in the BiSON-MDI combination  $p(H00|x) = 1.4 \times 10^{-3}$ . When a candidate was detected in more than one combination of data sets the minimum value of  $p(H00|x)$  is included in Table 2. In fact all of the included values of  $p(H00|x)$  were taken from the BiSON-GOLF combination, except for the g mode candidate, which was observed in the GOLF-MDI combination. However, unlike the  $l = 1, n = 9, m = -1$  candidate, some mode candidates were observed to be more prominent in the BiSON-MDI combination than in the GOLF-MDI combination. For example, the  $l = 1, n = 8, m = -1$  mode candidate was found to have a posterior probability of  $7.4 \times 10^{-8}$  when observed in the BiSON-MDI combination and  $6.6 \times 10^{-7}$  when observed in the GOLF-MDI combination. It should be noted that all of the results described in this section were dependent on the assumptions made when determining  $p(H00|x)$ . Different initial assumptions may have led to different results.

#### 7.4 Results of searching smoothed spectra with Bayesian statistics

As previously mentioned it is likely that the power of the p modes is spread over more than one frequency bin. Furthermore, García et al. (2007) found evidence that could suggest that g modes have short lifetimes, and so g-mode powers could also be spread across more than one frequency bin. With this in mind we have used Bayesian techniques to search smoothed frequency-power spectra.

We have used the methods described in Section 4.3 to search smoothed frequency-power spectra. We have then used equation (12) to determine the posterior probability. Again the frequency-power spectra were searched in pairs with one time series shifted to start 24 h after the other.

Fig. 11 shows the results of searching the BiSON, GOLF and MDI data when the frequency-power spectra were smoothed over various numbers of bins (all even values between 2 and 20). The uneven prior has been applied and removes 17 false detections, some of which can be attributed to daily harmonics and spacecraft frequencies.

Table 3 contains the frequencies of the observed mode candidates. Notice that the number of bins we needed to smooth over,  $R$ ,

**Table 3.** Candidates found when using Bayesian statistics to search smoothed spectra.  $R$  is the number of bins we have smoothed over.

$l$	$n$	$m$	Frequency ( $\mu\text{Hz}$ )	Minimum Posterior probability [ $P(\text{H}00 x)$ ]	$R$ at which minimum $P(\text{H}00 x)$ obtained	Distance from model frequency ( $\mu\text{Hz}$ )
0	7	0	$1120.01 \pm 0.05$	$4.4 \times 10^{-3}$	14	1.62
1	7	-1	$1182.64 \pm 0.02$	$5.4 \times 10^{-3}$	12	2.82 <sup>a</sup>
1	7	-1	$1185.17 \pm 0.02$	$1.2 \times 10^{-3}$	12	0.29 <sup>a</sup>
2	7	-2	$1244.90 \pm 0.06$	$1.3 \times 10^{-3}$	16	5.07 <sup>b</sup>
0	8	0	$1259.08 \pm 0.05$	$7.2 \times 10^{-3}$	14	4.52
1	8	-1	$1329.17 \pm 0.08$	$6.4 \times 10^{-25}$	20	
1	8	+1	$1329.93 \pm 0.08$	$4.2 \times 10^{-4}$	20	
		mean	$1329.55 \pm 0.11$			0.36
2	8	-2	$1393.87 \pm 0.07$	$1.3 \times 10^{-4}$	18	0.34 <sup>b</sup>
0	9	0	$1407.36 \pm 0.08$	$2.4 \times 10^{-12}$	18	0.63 <sup>b</sup>
1	9	-1	$1472.43 \pm 0.04$	$8.2 \times 10^{-18}$	10	
1	9	+1	$1473.19 \pm 0.07$	$2.5 \times 10^{-12}$	18	
		mean	$1472.81 \pm 0.08$			0.38

<sup>a</sup>Difference with model frequency assumes the  $m = -1$  component lies  $\pm 0.4 \mu\text{Hz}$  from central frequency.

<sup>b</sup>Difference with model frequency assumes  $m = -2$  components lies  $\pm 0.8 \mu\text{Hz}$  from central frequency.

**Table 2.** Candidates found using Bayesian statistics.

$l$	$n$	$m$	Frequency ( $\mu\text{Hz}$ )	Posterior probability [ $p(\text{H}00 x)$ ]	Distance from model frequency ( $\mu\text{Hz}$ )
2	-2	+2	$258.916 \pm 0.002$	$7.0 \times 10^{-3}$	1.236
0	6	0	$972.613 \pm 0.002$	$4.2 \times 10^{-3}$	0.132
1	7	-1	$1185.197 \pm 0.005$	$5.1 \times 10^{-4}$	0.256 <sup>a</sup>
0	8	0	$1263.209 \pm 0.007$	$6.2 \times 10^{-4}$	0.397
1	8	-1	$1329.235 \pm 0.005$	$4.5 \times 10^{-13}$	0.273 <sup>a</sup>
2	8	-2	$1393.872 \pm 0.007$	$3.6 \times 10^{-3}$	0.336 <sup>b</sup>
1	9	-1	$1472.433 \pm 0.008$	$1.6 \times 10^{-7}$	
1	9	+1	$1473.270 \pm 0.009$	$1.9 \times 10^{-4}$	
		mean	$1472.852 \pm 0.006$		0.34

<sup>a</sup>Difference with model frequency assumes the  $m = -1$  component lies  $\pm 0.4 \mu\text{Hz}$  from central frequency.

<sup>b</sup>Difference with model frequency assumes  $m = -2$  components lies  $\pm 0.8 \mu\text{Hz}$  from central frequency.

to minimize the observed posterior probability,  $P(\text{H}00|x)$ , is reasonably large (column 5). This highlights the truly resolved nature of the p mode profiles in the frequency-power spectra. Theoretically, the minimum value of  $p(\text{H}00|x)$  will occur when  $R$  is equal to the linewidth of the mode (Appourchaux et al. 2009). As can be seen in Table 3  $R$  does, in general, decrease with mode frequency. However, there are quite a few cases where this is not the case. This could be because we are looking for modes whose powers are only marginally greater than the background noise. Consequently, the mode profiles are difficult to distinguish from the noise, particularly in the limbs of the profiles and so the widths of the modes remain uncertain. The errors on the frequencies, given in Table 3, are the bin width of the smoothed spectra in which the minimum proba-

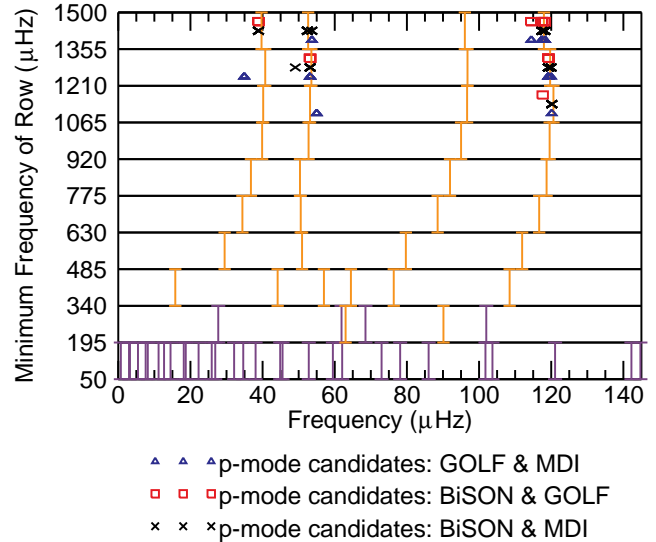


**Figure 11.** An echelle plot, modulo  $145 \mu\text{Hz}$ , marking locations in frequency of occurrences uncovered by the Bayesian test searches of smoothed spectra. The frequency-power spectra were smoothed over two, four, six, eight, 10, 12, 14, 16, 18 and 20 bins. The different symbols represent the different pairings of data that were searched (see legend).

bilities were observed (i.e.  $0.004R \mu\text{Hz}$ ). These error estimates are significantly larger than those given in Table 2.

Although formally allowed by the uneven prior, we regard any detections that are further than  $1 \mu\text{Hz}$  from the predicted frequencies with suspicion as, in general, the difference is significantly less than this. Notice that there are two  $l = 1, n = 7, m = -1$  candidates and two  $l = 0, n = 8$  candidates. In each case the candidate that lies closest to the predicted mode frequency also has the lowest posterior probability and so these candidates are more likely to represent the actual modes. No g-modes candidates were detected regardless of the assumed width and power. Once again we note

that the results described in this section are dependent on the initial assumptions made when using the Bayesian approach.

## 8 DISCUSSION OF THE RESULTS

We begin by comparing the results observed in the unsmoothed spectra using frequentist and Bayesian search methods. The frequencies of candidates that are detected by both approaches show very good agreement with each other and with previously claimed detections (see e.g. Toutain et al. 1998; Bertello et al. 2000; García et al. 2001; Chaplin et al. 2002; Broomhall et al. 2007; Salabert et al. 2009). When the frequentist approach was applied, more false detections (i.e. detections that were found to lie away from the predicted mode frequencies) were observed than expected. We believe this is significant and highlights the misleading nature of the frequentist approach. When the Bayesian approach was applied significantly fewer false detections were observed, even before the uneven prior probability was applied. Furthermore, the Bayesian approach allows us to use our knowledge of the Sun in a statistically rigorous manner to guide the frequencies at which we consider detections to be mode candidates (with the uneven prior probability). Although Bayesian methods may lead to more stringent threshold levels and consequently fewer detections we feel that this is a small price to pay for the improved accuracy and confidence one achieves in any detections. It is possible that using the uneven prior probability may discount detections that are in fact real mode signatures (type II errors). However, we feel that use of the uneven prior probability is justified as it also helps to minimize the number of noise signatures that are considered as mode candidates (type I errors). The Bayesian approach is also less open to misinterpretation than the frequentist approach. However, once again we note that the Bayesian approach is reliant on the assumptions made when determining the posterior probability. Different assumptions may lead to different mode candidates being uncovered. For example, the assumption that the rotational splitting of  $g$  modes is  $0.4 \mu\text{Hz}$  may be incorrect (García et al. 2007).

Mode candidates were also detected in smoothed spectra. This method was particularly successful at higher frequencies, where the modes have broader widths. It is worth noting that as the  $p$ -mode powers and widths were determined by extrapolation it is likely that the values used here are more accurate higher in the frequency search range. This may have influenced the results especially if the mode widths were overestimated. We were able to eliminate mode candidates that were positioned away from the predicted mode frequencies by employing the non-uniform prior probability. This cannot be done for the frequentist approach as we are effectively using a priori knowledge to guide the regions in frequency we search. The use of a priori knowledge in a statistically rigorous manner can only be done through Bayesian statistics.

The  $g$ -mode candidate that was observed in the frequentist approach was not detected when Bayesian statistics were used. One  $g$  mode candidate was detected using the Bayesian approach. However, each detection was only made in one combination of the data sets and neither candidate was detected with both the frequentist and Bayesian approaches. Therefore, we regard these two candidates with suspicion and feel that each candidate still requires further investigation and independent confirmation. The candidate that was detected with the Bayesian approach was not detected when the spectra were smoothed. This could indicate that, if it is a  $g$  mode, it has a lifetime that is longer than the lifetimes assumed here.

## ACKNOWLEDGEMENTS

The authors thank S. Basu and A. Serenelli for the solar models that were used to produce Fig. 2. We would like to thank all members of the Phoebus collaboration for much valued discussions concerning this work. This paper utilizes data collected by the Birmingham Solar-Oscillations Network (BiSON). We thank the members of the BiSON team, both past and present, for their technical and analytical support. We also thank P. Whitelock and P. Fourie at SAAO, the Carnegie Institution of Washington, the Australia Telescope National Facility (CSIRO), E.J. Rhodes (Mt. Wilson, California) and members (past and present) of the IAC, Tenderize. BiSON is funded by the Science and Technology Facilities Council (STF). The authors also acknowledge the financial support of STF. We thank the referee for insightful comments.

## REFERENCES

- Appourchaux T., 2004, *A&A*, 428, 1039  
 Appourchaux T., 2008, *Astron. Nachr.*, 329, 485  
 Appourchaux T., et al., 2000, *ApJ*, 538, 401  
 Appourchaux T., et al., 2010, *A&AR*, 18, 197  
 Appourchaux T., Samadi R., Dupret M., 2009, *A&A*, 506, 1  
 Bahcall J. N., Serenelli A. M., Basu S., 2006, *ApJS*, 165, 400  
 Belkacem K., Samadi R., Goupil M. J., Dupret M. A., Brun A. S., Baudin F., 2009, *A&A*, 494, 191  
 Berger J., Sellke T., 1987, *J. American Statistical Association*, 82, 112  
 Bertello L., et al., 2000, *ApJ*, 535, 1066  
 Broomhall A. M., Chaplin W. J., Elsworth Y., Appourchaux T., 2007, *MNRAS*, 379, 2  
 Broomhall A. M., Chaplin W. J., Elsworth Y., Fletcher S. T., 2008, *Astron. Nachr.*, 329, 461  
 Chaplin W., Elsworth Y., Isaak G., Marchenkov K., Miller B., New R., Pinter B., 2002, *MNRAS*, 336, 979  
 Chaplin W. J., Elsworth Y., Howe R., Isaak G. R., McLeod C. P., Miller B. A., New R., 1997, *MNRAS*, 287, 51  
 Chaplin W. J., Elsworth Y., Isaak G. R., Miller B. A., New R., 1999, *MNRAS*, 308, 424  
 Chaplin W. J., Serenelli A. M., Basu S., Elsworth Y., New R., Verner G. A., 2007, *ApJ*, 670, 872  
 Christensen-Dalsgaard J., Berthomieu G., 1991. *Solar interior and atmosphere*. Univ. of Arizona Press, Tucson, AZ, pp 401–478  
 Elsworth Y., Howe R., Isaak G. R., McLeod C. P., Miller B. A., New R., Speake C. C., Wheeler S. J., 1994, *MNRAS*, 269, 529  
 Fletcher S. T., Chaplin W. J., Elsworth Y., Schou J., Buzasi D., 2006, *MNRAS*, 371, 935  
 Gabriel A. H., et al., 2002, *A&A*, 390, 1119  
 García R. A., et al., 2001, *Sol. Phys.*, 200, 361  
 García R. A., et al., 2004, *Sol. Phys.*, 220, 269  
 García R. A., et al., 2005, *A&A*, 442, 385  
 García R. A., et al., 2008, *Astron. Nachr.*, 329, 476  
 García R. A., Mathur S., Ballot J., Eff-Darwich A., Jiménez-Reyes S. J., Korzenik S. G., 2008, *Sol. Phys.*, 251, 119  
 García R. A., Turck-Chièze S., Jiménez-Reyes S. J., Ballot J., Pallé P. L., Eff-Darwich A., Mathur S., Provost J., 2007, *Sci.*, 316, 1591  
 Houdek G., Balmforth N. J., Christensen-Dalsgaard J., Gough D. O., 1999, *A&A*, 351, 582  
 Mathur S., Eff-Darwich A., García R. A., Turck-Chièze S., 2008, *A&A*, 484, 517  
 Mathur S., Turck-Chièze S., Couvidat S., García R. A., 2007, *ApJ*, 668, 594  
 Provost J., Berthomieu G., Morel P., 2000, *A&A*, 353, 775  
 Salabert D., Leibacher J., Appourchaux T., Hill F., 2009, *ApJ*, 696, 653  
 Scherrer P. H., et al., 1995, *Sol. Phys.*, 162, 129  
 Sellke T., Bayarri M., Berger J., 2001, *The American Statistician*, 55, 62  
 Sturrock P. A., 2008, arXiv:0809.0276v1

Toutain T., Appourchaux T., Fröhlich C., Kosovichev A. G., Nigam R.,  
Scherrer P. H., 1998, *ApJ*, 506, L147  
Turck-Chièze S., et al., 2001, *ApJ*, 555, L69  
Turck-Chièze S., et al., 2004, *ApJ*, 604, 455  
Zaatri A., Provost J., Berthomieu G., Morel P., Corbard T., 2007, *A&A*,  
469, 1145

**APPENDIX A: TABLE OF ASSUMPTIONS****Table A1.** Assumptions made with each approach.

Property	Frequentist	Bayesian
Underlying statistics	Gaussian (for frequency-amplitude spectra)	$\chi^2$ 2d.o.f. (for frequency-power spectra)
Threshold probability	0.01	0.01
Rotational splitting	$0.4 \mu\text{Hz}$	$0.4 \mu\text{Hz}$
Power of p modes	None	Based on extrapolations (see Section 4.1): $0.1 \text{ mm}^2 \text{ s}^{-2} \leq V^2 \leq 38 \text{ mm}^2 \text{ s}^{-2}$
Power of g modes	None	Based on models (see Section 4.1): $V^2 = 9$ or $36 \text{ mm}^2 \text{ s}^{-2}$
Frequencies considered as p-mode candidates	Closer than $1 \mu\text{Hz}$ to a model mode frequency	Allowed by uneven prior probability i.e. an inverted top-hat distribution, based on frequencies predicted by 5000 models
Frequencies considered as g-mode candidates	Closer than $1 \mu\text{Hz}$ to a model mode frequency	Allowed by uneven prior probability i.e. an inverted top-hat distribution, based on frequencies predicted by models and an uncertainty of 1 per cent
Lifetimes of p modes	Long enough for the power to be confined to a few bins only	Based on extrapolations (see Section 4.1) $795 \text{ d} \geq \tau \geq 35 \text{ d}$
Lifetimes when searching for g-mode single spikes	Greater than the length of the time series i.e. $\tau > 3071 \text{ d}$ .	Greater than the length of the time series i.e. $\tau > 3071 \text{ d}$
Lifetimes when searching for g-mode peaks	1, 2, 3, and 4 months	1, 2, 3, and 4 months